Nonlocal optical effects on the fluorescence and decay rates for admolecules at a metallic nanoparticle

Jason Vielma and P. T. Leung[a)]
Department of Physics, Portland State University, P.O. Box 751, Portland, Oregon 97207-0751

(Received 26 January 2007; accepted 28 March 2007; published online 16 May 2007)

A phenomenological model is implemented to study the decay rates of fluorescing molecules in the vicinity of a metallic nanoparticle, wherein the nonlocal optical response of the particle is accounted for via the hydrodynamic model for the description of the free electrons in the metal. These nonlocal effects are examined for each of the radiative rate and the nonradiative rate of the admolecule, respectively. In addition, the overall fluorescence rate which includes the enhancement ratio for the driving field intensity is also studied. It is found that for particles of very small sizes (<10 nm), the nonlocal effects, in general, lead to significantly greater fluorescence rates and smaller nonradiative decay rates for the admolecules, with the effects on radiative rates depending crucially on the orientation of the molecules. Furthermore, the effects are mostly noticeable for molecules close to the metal particle and in processes where higher multipolar interactions are significant such as those in nonradiative decay processes. Above all, these nonlocal effects can still be observable in the presence of large surface damping imposed on the metallic electrons due to the ultrasmall sizes of these nanoparticles. The relevance of these effects to some of the latest experiments is discussed.
 [DOI: 10.1063/1.2734549]

I. INTRODUCTION

The study of molecular fluorescence near a metallic boundary has been an active area of research since the 1970s.[1] Recently, due to the advances both in nanoparticle plasmonics and in experiments with single molecules, several significant experiments have been carried out in the study of single-molecule fluorescence at a single metallic nanoparticle.[2–5] In some earlier experiments,[4,5] Dulkeith *et al.* have studied the quenching of fluorescence (i.e., decrease in quantum yield) for dye molecules chemically attached to gold nanoparticles (AuNP's) of sizes with radius (a) down to 1 nm. They have accounted for such decrease in quantum yield being originated from a decrease in radiative rate (for tangentially oriented molecules) and increase in nonradiative rate for the admolecules near the AuNP. They have further carried out a detailed study of the various decay rates as a function of the molecule-particle distance (d) and have concluded that the classical phenomenological (CP) model can only offer a qualitative account of their experimental results.

In the two more recent studies,[2,3] AuNP's of greater sizes ($2a \sim 100$ nm) act as nanoantennas are being used to scan over thin films spin coated with a very low concentration of emitting molecules. In contrast to the experiments by Dulkeith *et al.*, the molecules in these later experiments are determined to have almost radial orientation with respect to the AuNP. Furthermore, these later experiments have not only studied the quantum yield (fraction of radiative rate over total decay rate) but also the overall fluorescence yield, which incorporates the field enhancement factor due mainly to the surface plasmon excitation from the AuNP. Both groups have observed an enhancement of fluorescence yield at close distances (d), and they accounted for this by referring to the field enhancement and the increase in radiative rates for radial oriented molecules. In addition, Anger *et al.*[2] have observed the existence of an optimal distance (d_{op}) at which the fluorescence yield is maximum, where such d_{op} emerges from the competition between the field enhancement and the quenching of the quantum yield for the molecule.[6] Moreover, both groups have found that for AuNP of such a relatively large size, the CP model is applicable and fits well with the results obtained in their experiments.

Theoretically, the problems of both the enhanced fields and the molecular decay rates at a metallic nanoparticle have been studied from time to time for more than three decades, starting with the discovery of the dramatic surface enhanced spectroscopy in the vicinity of metallic nanostructures in the 1970s.[7] Models from the CP ones[8–12] to quantum mechanical (QM) ones[13–15] have been implemented over the years. While the optical fields are most of the time treated classical in these models; the molecule and the metallic structure can have both CP and QM formulations. For example, the molecule has been previously described in the literature from using the simple model of a classical harmonic point dipole[1,8–13] to QM descriptions using density functional theories (DFTs);[14,15] the metal particle has also been described from merely focusing on its macroscopic electromagnetic dielectric response[1,8–12] to a DFT description of the metallic electrons.[13] Even most recently, both approaches have still been adopted by different researchers, as can been seen from the very recent work of Carminati *et al.*[16] who have performed a detailed study of the distance dependence of the various radiative and nonradiative molecular decay rates using a CP approach; while as mentioned above, an Italian

a)Electronic mail: hopl@pdx.edu

group has in some very recent studies implemented a QM description for the molecules.[14,15] This latter group has further extended their model to treat metallic particles of arbitrary shapes (as aggregates of interlocking spheres) and to account for the enhanced excitation of the molecule in the presence of the metal particle. However, there still exist uncompromising comparisons between these latest calculated results and experimental data,[4,5,14,15] especially in the "close distance regime" (and for ultrasmall particles) when the molecule is almost on the surface of the metal particle. When being close to the metal surface, the wave nature of the surface electrons may not be ignored and one may need to account for the quantum nature of the metal particle.

Among the common features in most of the above cited previous theoretical works,[8–12,14–16] they have all treated the metal particle classically via its macroscopic dielectric electromagnetic response. The only one[13] which has treated the metal particle quantum mechanically using DFT is, however, limited to only ultrasmall particles ($\sim$1–2 nm in diameter) due to the increasing demand of computational power for larger particles. However, QM effects at distances close to the metal surface can manifest up to $\sim$10 nm sizes of particles. Hence it will be of interest to account for (at least partially) these QM effects from the metal particle using a more realistic phenomenological approach for particle sizes up to $\sim$10 nm. One such approach is to introduce the nonlocal (NL) optical response of the metal particle into the theory of fluorescence. This NL approach will replace the dispersive dielectric function $\varepsilon(\omega)$ by one which has dependence on both the frequency and the wave vector $\varepsilon(\mathbf{k},\omega)$ so that QM effects of the metal can be introduced by adopting various QM models for this latter response function.[17]

In a previous work,[18] we have studied the total molecular decay rates using a nonlocal dielectric model and have obtained nontrivial effects for molecules very close to a metallic particle of ultrasmall sizes.[19] It is the purpose of our present work to extend this previous study to decipher these NL effects on each of the radiative and nonradiative rates for the admolecules.[20] In addition, we shall also study these effects on the overall fluorescence yield by incorporating the field enhancement effects. We will see that such NL effects will be significant for ultrasmall particles, close molecule-particle distances, and processes involving multipolar response of the particle such as that in the nonradiative rate calculations. In the literature, it appears that these NL effects might have been found to be relevant in some experiments with ultrasmall metal particles;[4] while the CP models without the NL response were found to already fit well in certain recent experiments with larger particles.[2,3] We shall see below that these NL effects can be significant even for large particles if the molecule is very close to it.

II. THEORETICAL FORMULATION

As described by Anger *et al.*,[2] the overall fluorescence yield depends on the product of two factors: the enhanced excitation field and the quantum yield of the dye in the vicinity of the metal particle. To be specific in our modeling study, we shall always consider the driving field to be in the same direction as the molecular dipole moment. Given this, we can then express the overall normalized fluorescence yield in the following form:[2]

$$\frac{\gamma^{\mathrm{FL}}}{\gamma_0^{\mathrm{FL}}} = \left|\frac{E}{E_0}\right|^2 \left(\frac{\gamma^{\mathrm{R}}}{\gamma^{\mathrm{R}}+\gamma^{\mathrm{NR}}}\right), \tag{1}$$

where the first term on the right hand side is the field enhancement ratio and the second term is the quantum yield defined as the ratio of the radiative to the total decay rates of the admolecule, with both rates being modified due to the interaction between the molecule and the metal particle. We shall consider an ideal free molecule with intrinsic quantum yield assumed to be unity. Furthermore, we shall consider spherical metal particles with radius much smaller than the emission wavelengths ($a \ll \lambda$) as well as close molecule-particle distances $d \ll \lambda$. Under this long wavelength approximation, solutions from electrostatics can be applied in the CP description. Hence, for the two orthogonal orientations of the molecule located in vacuum outside the particle, we have the following results:[8]

A. For tangential molecular dipoles

$$\left|\frac{E}{E_0}\right|_{\parallel}^2 = \left|1 - \frac{\alpha_1}{(a+d)^3}\right|^2, \tag{2}$$

$$\frac{\gamma_{\parallel}^{\mathrm{R}}}{\gamma_0} = \left|1 - \frac{\alpha_1}{(a+d)^3}\right|^2, \tag{3}$$

$$\frac{\gamma_{\parallel}^{\mathrm{NR}}}{\gamma_0} = -\frac{3}{4}\left(\frac{c}{\omega a}\right)^3 \sum_n (n+1)(2n+1) \times \mathrm{Im}\left(\frac{1}{\varepsilon+(n+1)/n}\right)\left(\frac{a}{a+d}\right)^{2n+4}, \tag{4}$$

where $\alpha_1 = [(\varepsilon-1)/(\varepsilon+2)]a^3$ is the dipole polarizability of the sphere with $\varepsilon(\omega)$ being the local dielectric function of the metal particle. Note that we have adopted the Gersten-Nitzan (GN) model[8] where the normalized radiative rate is computed from the Poynting vector of the emitted dipolar field from the molecule-sphere system; while the nonradiative rate is computed from the Joule loss due to absorption of the emission by the metal particle. On the other hand, one can also calculate directly the total decay rate $\gamma^{\mathrm{TOTAL}} = \gamma^{\mathrm{R}} + \gamma^{\mathrm{NR}}$ from a damped harmonic oscillator model[1] and obtain the following result for the normalized rate:[11,18,20]

$$\frac{\gamma_{\parallel}^{\mathrm{TOTAL}}}{\gamma_0} = 1 + \frac{3}{4}\left(\frac{c}{\omega}\right)^3 \sum_n n(n+1)\frac{\mathrm{Im}\,\alpha_n}{(a+d)^{2n+4}}, \tag{5}$$

with the multipole polarizability of the sphere defined as

$$\alpha_n = \frac{\varepsilon-1}{\varepsilon+(n+1)/n} a^{2n+1}. \tag{6}$$

In this latter approach, the nonradiative rate can then be obtained from the difference between Eqs. (5) and (3), and the result should, in principle, check with that obtained from Eq. (4).[21]

B. For radial molecular dipoles

In a similar way, we can obtain the following results for a radial-oriented molecule:

$$\left|\frac{E}{E_0}\right|_{\perp}^2 = \left|1+\frac{2\alpha_1}{(a+d)^3}\right|^2, \tag{7}$$

$$\frac{\gamma_{\perp}^{R}}{\gamma_0} = \left|1+\frac{2\alpha_1}{(a+d)^3}\right|^2, \tag{8}$$

$$\frac{\gamma_{\perp}^{NR}}{\gamma_0} = -\frac{3}{2}\left(\frac{c}{\omega a}\right)^3 \sum_n (2n+1)\frac{(n+1)^2}{n} \times \mathrm{Im}\left(\frac{1}{\varepsilon+(n+1)/n}\right)\left(\frac{a}{a+d}\right)^{2n+4}, \tag{9}$$

$$\frac{\gamma_{\perp}^{TOTAL}}{\gamma_0} = 1+\frac{3}{2}\left(\frac{c}{\omega}\right)^3 \sum_n (n+1)^2 \frac{\mathrm{Im}\,\alpha_n}{(a+d)^{2n+4}}. \tag{10}$$

We note that in this simple CP long wavelength approximation, the multipolar response of the sphere occurs only in the nonradiative and total decay rates, but not in the field enhancement ratio or in the radiative decay rate—where only dipolar response appears. Thus, using Eqs. (2)–(10) into Eq. (1), we can compute the normalized fluorescence yield for each of the two orientations of the molecule near the metal particle.

To study the effects due to the nonlocal response of the metal sphere, we applied the previous work of Fuchs and Claro,[22] in which the NL multipole polarizability of a sphere has been derived in the semiclassical infinite barrier (SCIB) approximation and can be expressed in the following form:

$$\alpha_n^{NL} = \frac{\xi_n - 1}{\xi_n + (n+1)/n} a^{2n+1}, \tag{11}$$

where the "effective dielectric function" is given by

$$\xi_n(\omega) = \left[\frac{2}{\pi}(2n+1)a\int_0^{\infty}\frac{j_n^2(ka)}{\varepsilon(k,\omega)}dk\right]^{-1}, \tag{12}$$

with j_n the spherical Bessel function, and we have assumed isotropic nonlocal dielectric response. Using the simple hydrodynamic model for $\varepsilon(k,\omega)$, Eq. (12) can be integrated to obtain:[22]

$$\xi_n(\omega) = \left[\frac{1}{\varepsilon_D} + (2n+1)\left(\frac{a\omega_P}{\beta u}\right)^2 I_{n+1/2}(\omega)K_{n+1/2}(\omega)\right]^{-1}, \tag{13}$$

where ω_P is the bulk plasmon frequency, I and K are the modified Bessel functions, β and u are parameters as defined in Ref. 22, and the Drude dielectric function is given by $\varepsilon_D = 1-\omega_P^2/(\omega^2+i\omega\Gamma)$, with Γ being modified from the bulk damping constant to include surface scattering effects.[23] Thus, using Eq. (11) to replace the local polarizability that appears in Eqs. (2), (3), (5), (7), (8), and (10); as well as Eq. (13) to replace the dielectric function in Eqs. (4) and (9), we can then study the NL effects on the various decay and fluorescence rates. In the following, we shall perform such numerical study and compare the results with respect to those from using the Drude model as the local dielectric response in the corresponding equations.

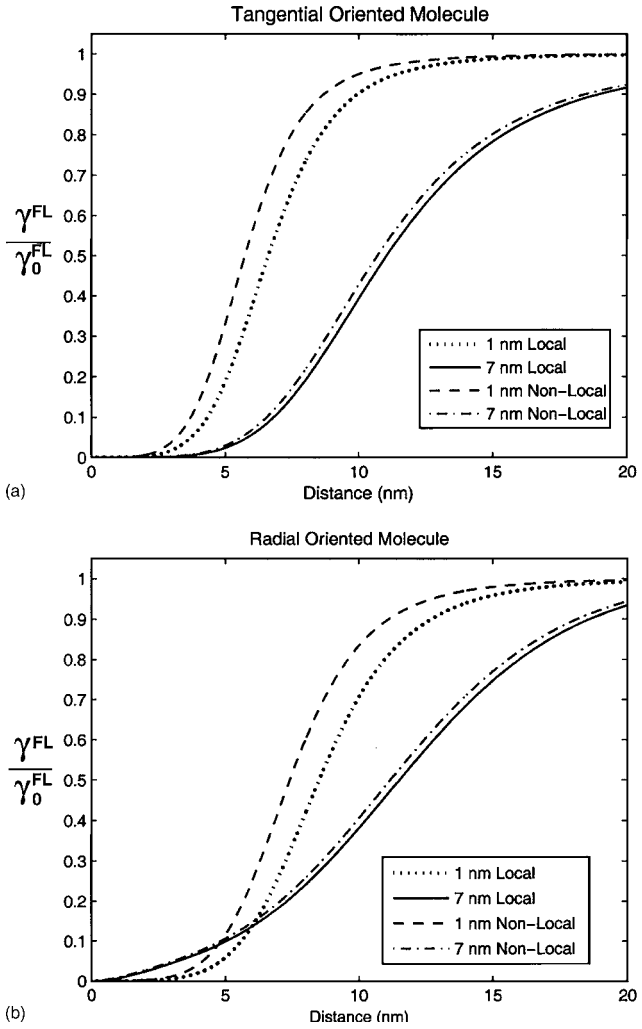

FIG. 1. Normalized fluorescence yield as a function of the distance of the molecule from a gold nanosphere of two different sizes (radii of 1 and 7 nm) for (a) the tangential and (b) the radial orientation of the molecular dipole according to the Drude (local) and the hydrodynamic model (nonlocal) at an emission wavelength of 650 nm.

III. NUMERICAL RESULTS

To demonstrate the possible NL effects, we have performed several model calculations with the metallic nanoparticle taken as an ultrasmall gold nanosphere of radius $a \lesssim 10$ nm. The various parameters for gold are taken from Ref. 24, with the Drude damping rate for the free electrons given by $\Gamma = \Gamma_{BULK} + Av_F/a$, i.e., a sum of the bulk and surface damping rates, where v_F is the Fermi velocity of the metal and A is a constant of order unity.

Figure 1 shows the results for the fluorescence yield [Eq. (1)] of a molecule emitting in the vicinity of a nanosphere of two different sizes (a), as a function of molecule-particle distance (d). Both molecular orientations are considered. It is seen that no enhancement of fluorescence yield is possible for such small metal particles, with the nonradiative decay dominates significantly over the field enhancement at close

distances.[2] Furthermore, the latter drops so rapidly with distance that an optimal distance does not show up as the molecule is moved away from the particle. This is consistent with that reported in Ref. 2, in which an optimal distance shows up only for $a>10$ nm. It is clearly seen that the NL effects are most significant for ultrasmall particles, leading to overall stronger fluorescence rates. For example, for a radial dipole at $d=1$ nm from the spheres, the NL effects lead to a rate about 1.8 times that from the local theory for the 1 nm sphere, and about 1.4 times as large for the 7 nm sphere. These effects still prevail at larger distances for these ultrasmall spheres. As an example, for a radial dipole at $d=10$ nm, the NL result yields an 18% increment for the 1 nm sphere and 6% for the 7 nm sphere. This occurs due to the significant drop in nonradiative rates from the NL effects (see below) in spite of the decrease in the field enhancement due also to these effects. For larger spheres such as those employed in Ref. 2, we found that (not shown in the figure) the NL effects are significant only for very close distances, for example, they can amount to 50% increase at $d=1$ nm for a 30 nm sphere for a radial dipole, but drop to only 0.6% at $d=10$ nm. Note that, though not obvious from the graphs, the significance of these NL effects goes down on the average with the increase in the distance d. Note also that the "tangential molecule" experiences a greater fluorescence yield, in general, due to the relatively large quantum yield, in spite of the fact that both the field enhancement and the radiative rate are smaller for this orientation of the molecule. This happens because of the much less nonradiative rate for tangential molecules. All these can be seen by comparing Eqs. (2)–(4) with Eqs. (7)–(9). However, the NL effects for the two molecular orientations are pretty consistent and comparable with each other.

Figure 2 shows the frequency spectrum of the fluorescence yield at a close molecule-particle distance of 1 nm. It is seen that while the surface plasmon peak ($\omega_{SP}\sim\omega/\sqrt{3}$) emerges clearly for the 7 nm particle, it disappears for the one with only 1 nm in radius. This happens since the dipolar resonance factor in the field enhancement and the radiative rate dominates only for $a\gg d$, for small values of $a\sim d$, this dipolar resonance will be overshadowed by the multipolar terms in the nonradiative rate, as can be understood from examining Eqs. (2)–(4) and Eqs. (7)–(9). Furthermore, the familiar blueshift in the resonance peaks can be observed in all cases: for both the particles and the two different molecular orientations. This blueshift in surface plasmon resonances is well known within the SCIB model for the NL response of the metal spheres.[18,19,22,25] Note also the "opposite behaviors" in the "anomalous dispersion" patterns for the radiative rates in the two orthogonal orientations of the molecule. Figure 3 shows the fluorescence yield as a function of the particle radius at different molecule-particle distances. It is seen that the NL effects again lead to higher overall yield and, in general, become less significant for larger particles. In addition, no optimum particle radius is observed, for which the fluorescence is maximized given other factors fixed. Moreover, we see that while the tangential dipole shows a monotonic decrease in fluorescence as the radius a increases, the radial one behaves quite differently with the overall yield

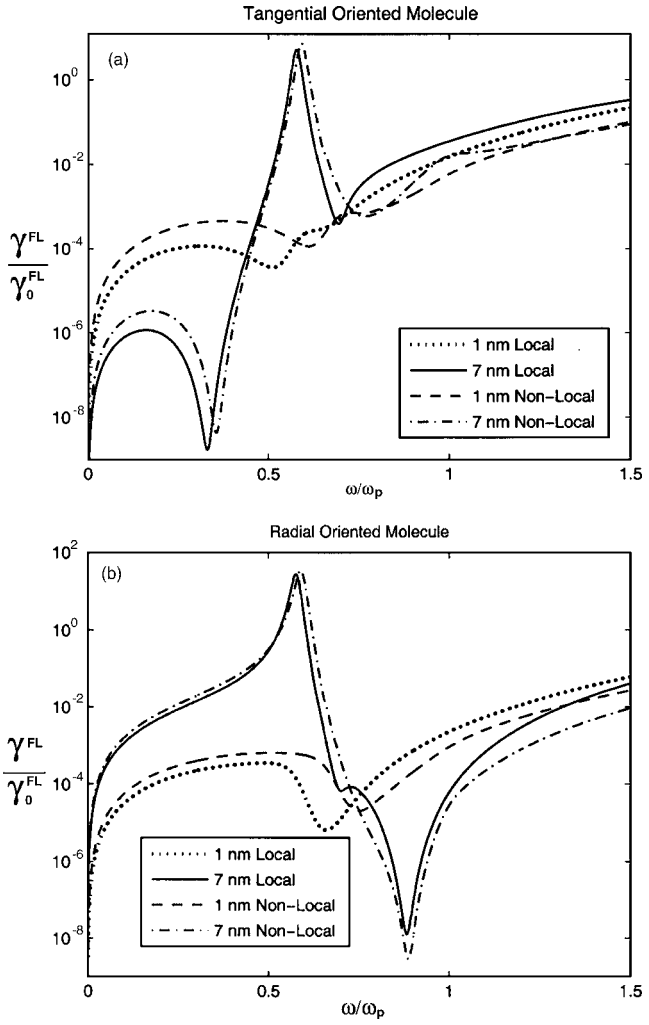

FIG. 2. Frequency spectrum of the normalized fluorescence yield as a function of the emission frequency of the molecule (in units of the metal plasmon frequency) at a distance of 1 nm from the gold nanosphere. Other labels are same as in Fig. 1.

rises with a after passing a certain minimum value, yielding an overall enhanced fluorescence yield for farther molecule-particle distances. This can be understood again in terms of the competition among the three factors (i.e., field enhancement, radiative rate, and nonradiative rate), as discussed above. Due to the relatively "weak effect" combined from the field enhancement and the radiative rate decrease for the tangential dipole, one ends up with an overall decrease of fluorescence yield as the particle becomes larger.

Since so far as we are aware, only decay rate (lifetime quenching) experiments have been conducted with ultrasmall ($a<10$ nm) metal particles,[4,5,26] we shall next study explicitly the NL effects on these decay rates. Figures 4–6 show the effects on each of the radiative and nonradiative rates for the AuNP studied in Ref. 5. We find that very close values are obtained for the calculation of the nonradiative rates, from either direct consideration of energy absorption in the metal particle [Eqs. (4) and (9)] or from the difference between the total and radiative rates.[21] Overall, we see that the general qualitative trends in all these graphs agree reasonably with the previous results from experiments[4,5] as well as those from quantum mechanical calculations[14,15] for tangentially

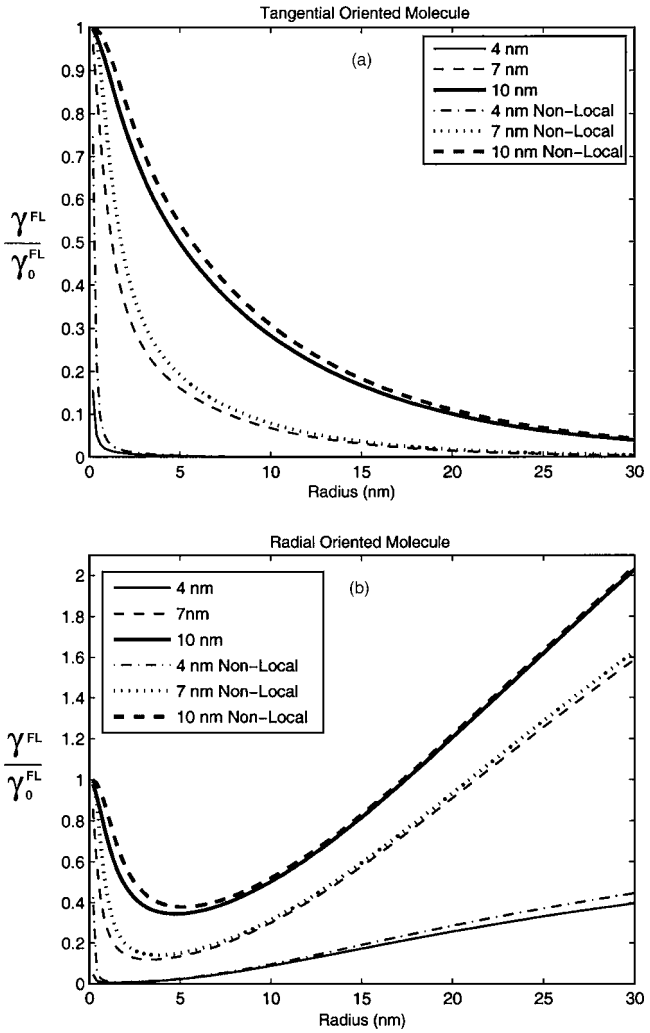

FIG. 3. Same as in Fig. 1, except that the fluorescence yield is plotted as a function of the sphere radius for several molecule-sphere distances at 4, 7, and 10 nm, respectively.

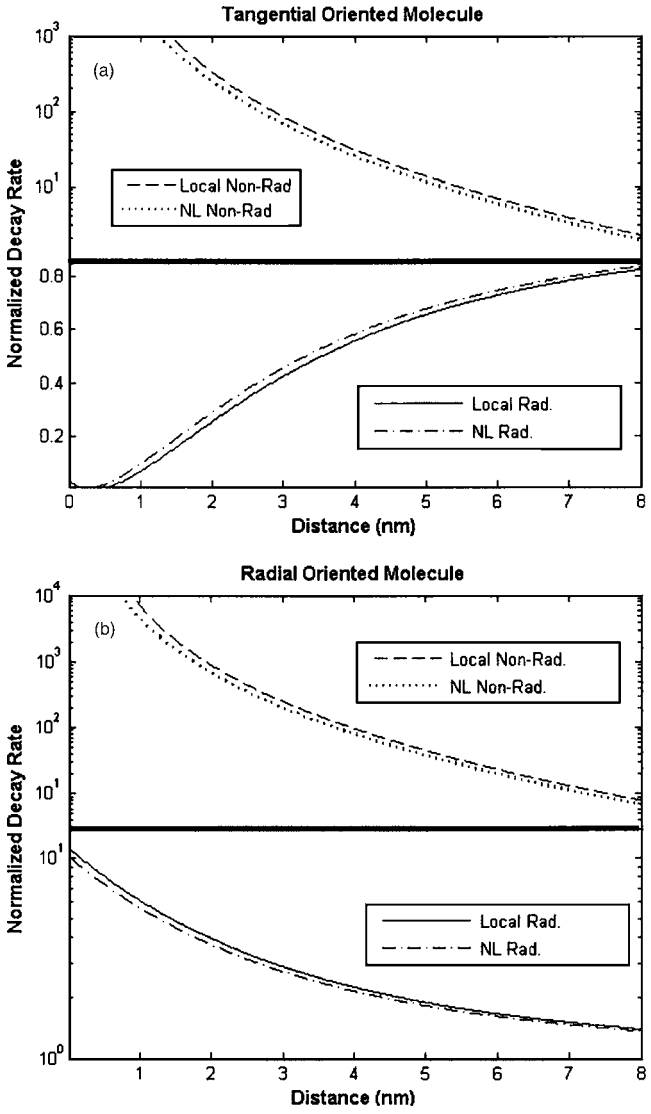

FIG. 4. Normalized radiative and nonradiative decay rates as a function of the distance from a gold nanosphere of 6 nm radius and at an emission wavelength of 650 nm, for (a) the tangential and (b) the radial orientation of the molecular dipole according to the Drude (local) and the hydrodynamic model (nonlocal).

oriented molecules. We note that for emission frequency below the surface plasmon resonance (SPR) of the metal particle, the decay rates are, in general, smaller for tangential molecules. As a function of molecule-particle distance, it is found that the NL effects lower the decay rates for most cases at optical emission frequencies below SPR, except for the radiative rates of a tangential dipole. Except for this latter case, the NL effects lead to results deviated from the GN model in a direction closer to the experimental data,[4,5] a trend also achieved by treating the molecule quantum mechanically using DFT.[14,15] Figure 7 shows the reduction of the GN model by roughly an order of magnitude due to NL effects, calculated for exactly the same system, as in Fig. 4 of Ref. 14. Since the previous DFT calculation[14] already showed results an order of magnitude smaller than the GN model, it appears that if both these two effects (i.e., the quantum effects from both the molecule and the metal particle) can somehow be put together as was done previously by Corni and Tomasi (see Ref. 27) for the case of a planar metallic surface, the combined theoretical results would be even closer to the experimental data. Again, these effects are most prominent at close distances (Fig. 4) and/or small particle sizes (Fig. 6), where the emission frequency is fixed at $\omega \sim 0.22\omega_P$. Furthermore, we see that while the NL effects will become relatively insignificant as d becomes a little larger (>10 nm), they can prevail for particle sizes up to 30 nm in radius at very close distances. Aside from distance and particle size dependence, the frequency spectra showed in Fig. 5 demonstrate the familiar blueshift and the "relative reversed anomalous dispersion" in SPR for the two orthogonally oriented molecules as before. Finally, it is also noticeable in all the Figs. 4–6 that the NL effects are, in general, greater for nonradiative rates compared to those for radiative rates due to the prominence of multipolar interaction involved in the former decay process (note the different scales in some of the plots).

IV. DISCUSSION AND CONCLUSION

Within a phenomenological model, we have studied the possible quantum mechanical effects from a metallic nano-

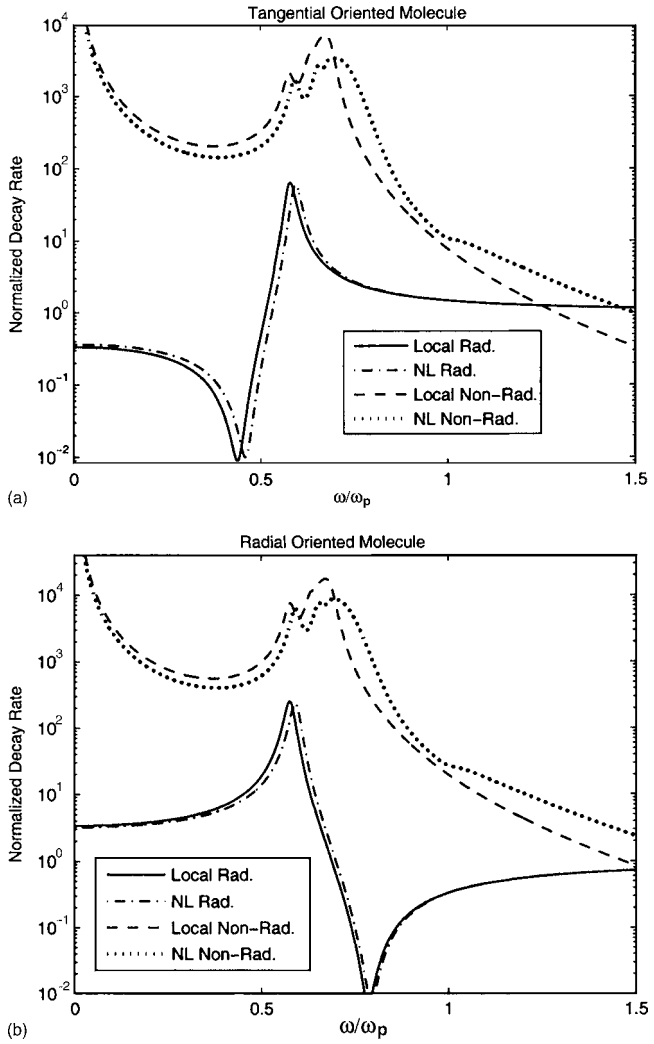

FIG. 5. Same as in Fig. 4, except that the frequency spectrum is plotted with the molecule-sphere distance fixed at 1 nm.

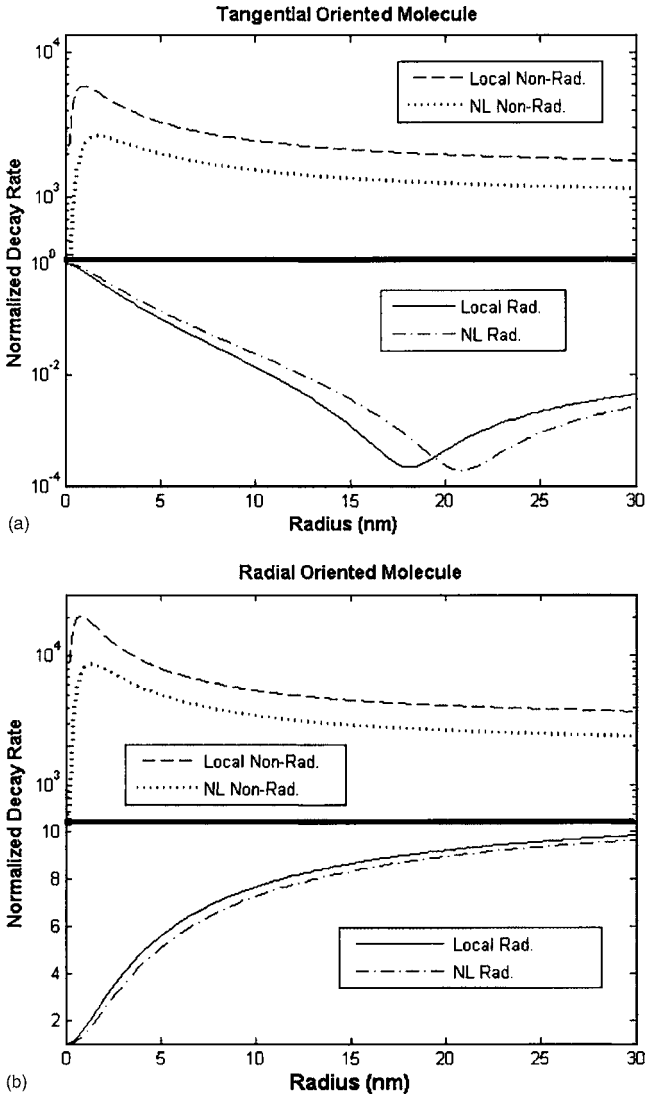

FIG. 6. Same as in Fig. 4, except the decay rates as a function of the radius of the gold sphere are plotted with a molecule-sphere distance fixed at 1 nm.

particle on the fluorescence yield and decay rates of an admolecule through the nonlocal optical response of the particle. These effects have been found to be significant for close molecule-particle distances as well as particles of ultrasmall sizes, and can lead to significantly higher fluorescence yield. For molecular decay rates, these effects modify both the radiative and nonradiative rates from the GN model in a direction bringing theory closer to experiments in several cases, except for the radiative rates of tangentially oriented molecules at frequencies below that of the SPR of the particle.

Improvements of the present model can be achieved by using more sophisticated quantum models for the nonlocal dielectric response of the metal such as the Lindhard-Mermin model.[17,22,27] In addition, in actual comparison with experiments, the interband transition due to the lattice binding effect on the electrons can always be accounted for by the addition of a constant to the free-electron dielectric function in the local theory (i.e., the Drude model).[24] It seems that this procedure can still be applied in the present nonlocal model which utilizes an effective local dielectric function [Eq. (12)] by integrating over the wave vectors. A more rigorous treatment of the interband transitions in the presence of

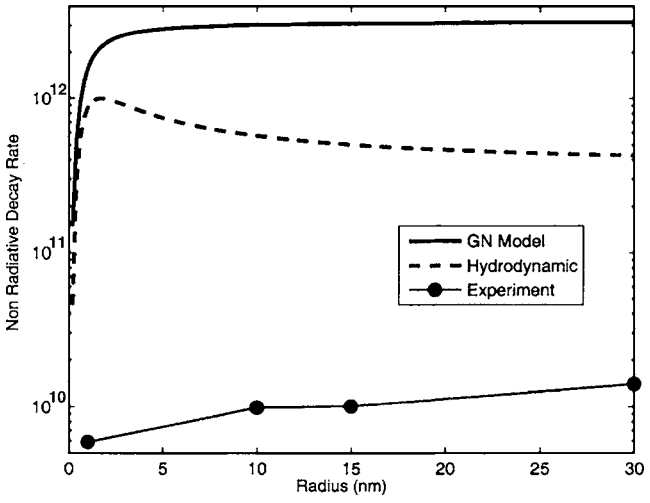

FIG. 7. Comparison between the local and nonlocal calculations for nonradiative rates (in s^{-1}) as a function of the sphere radius under the same conditions as those for Fig. 4 of Ref. 14. Also reproduced are the experimental data from Ref. 4 for comparison as done in Ref. 14.

nonlocal response would be very challenging. Furthermore, the separable form of the fluorescence yield into the field enhancement and the quantum yield factors in Eq. (1) will become inaccurate in the presence of nonlocal response from the metallic sphere at very close molecule-sphere distances, since this is derived by assuming the molecular dipole being driven by a local electric field. Modification of this separability leading to possible mixing of the two factors will be of great interest but highly nontrivial. Another improvement will be to go beyond the SCIB model to allow not only the electric field but also its derivatives (i.e., the electronic charge density) to be continuous across the geometric boundary of the sphere.[28] A more rigorous approach using random phase approximation has been previously formulated for the case of planar metallic boundaries.[29] This approach employs a dielectric function which is continuous across the geometric surface boundary, leading naturally to the continuity of both the fields and the charge density across the boundary. It will be of great interest to generalize this approach to spherical geometries so that the problem considered in the present work can be studied in a more rigorous way.

The present approach, though limited, does allow one to introduce, at least partially, the quantum effects in the optical response of the metal particle involved in a molecule-particle interacting system, without limitation to particles only of extremely small sizes. In contrast, other microscopic approaches such as those based on time-dependent density functional theory for the description of the metallic response are limited only to particles of sizes smaller than 1–2 nm due to heavily involved computations for larger particles. Thus our approach provides an "economical way" to study these possible "metallic quantum effects" which may survive for particles up to ~10 nm in radius, and for even larger spheres at very close molecule-particle distances. As remarked above, these effects could have played a role in the recent experiments with ultrasmall AuNP's;[4,5,26] and even in those with relatively larger spheres ($a \sim 10-50$ nm) (Refs. 2 and 3) when the molecule is excited at distances very close to the sphere. Moreover, it seems that up to the present time only molecular decay rate measurements have been performed with metal particles of ultrasmall sizes. It is thus of interest to also study experimentally the fluorescence yields for molecules in the vicinity of metal particles of a few nanometers in size, and see how the results compare with the modeling results from our present work.

ACKNOWLEDGMENT

This work is partially supported by a research grant from Intel corporation.

[1] R. R. Chance, A. Prock, and R. Silbey, Adv. Chem. Phys. **1**, 37 (1978).
[2] P. Anger, P. Bharadwaj, and L. Novotny, Phys. Rev. Lett. **96**, 113002 (2006).
[3] S. Kuhn, U. Hakanson, L. Rogobete, and V. Sandoghkar, Phys. Rev. Lett. **97**, 017402 (2006).
[4] E. Dulkeith, A. C. Morteani, T. Niedereichholz, T. A. Klar, J. Feldmann, S. A. Levi, F. C. J. M. van Veggel, D. N. Reinhoudt, M. Moller, and D. I. Gittins, Phys. Rev. Lett. **89**, 203002 (2002).
[5] E. Dulkeith, M. Ringler, T. A. Klar, J. Feldmann, A. Munoz Javier, and W. J. Parak, Nano Lett. **5**, 585 (2005).
[6] The presence of an optimal distance in such processes involving two competing mechanisms has been well known for a long time since the 1980s. See, e.g., P. T. Leung and T. F. George, J. Chem. Phys. **85**, 4729 (1986) and references therein.
[7] See, e.g., the earlier review articles by J. I. Gersten and A. Nitzan, Surf. Sci. **158**, 165 (1985) and by M. Moskovits, Rev. Mod. Phys. **57**, 783 (1985).
[8] J. Gersten and A. Nitzan, J. Chem. Phys. **75**, 1139 (1981), and the mathematical appendix to this paper: AIP Document No. PAPS JCP SA-75-1139-32, Section B. See also their above reference in Ref. 7.
[9] R. Ruppin, J. Chem. Phys. **76**, 1681 (1982).
[10] H. Chew, J. Chem. Phys. **87**, 1355 (1987).
[11] Y. S. Kim, P. T. Leung, and T. F. George, Surf. Sci. **195**, 1 (1988).
[12] P. C. Das and A. Puri, Phys. Rev. **65**, 155416 (2002).
[13] W. Ekardt and Z. Penzar, Phys. Rev. B **34**, 8444 (1986).
[14] O. Andreussi, S. Corni, B. Mennucci, and J. Tomasi, J. Chem. Phys. **121**, 10190 (2004).
[15] M. Caricato, O. Andreussi, and S. Corni, J. Phys. Chem. B **110**, 16652 (2006).
[16] R. Carminati, J. J. Greffet, C. Henkel, and J. M. Vigoureux, Opt. Commun. **261**, 368 (2006).
[17] See, e.g., G. D. Mahan, *Many-Particle Physics*, 3rd ed. (Plenum, New York, 2000), Sec. 5.5.
[18] P. T. Leung, Phys. Rev. B **42**, 7622 (1990).
[19] A similar study has been carried out even earlier by other researchers using a slightly different approach based on the Green dyadic formulation, see G. S. Agarwal and S. V. O'Neil, Phys. Rev. B **28**, 487 (1983). The corresponding effects on the emission frequency of the molecule was also studied in P. T. Leung, and M. H. Hider, J. Chem. Phys. **98**, 5019 (1993).
[20] A very comprehensive review up to our previous work in Ref. 18 was recently published by J. I. Gersten. The review entitled "Theory of fluorophore-metallic surface interactions" can be found in *Trends in Fluorescence Spectroscopy*, edited by C. D. Geddes and J. Lakowicz (Springer, New York, 2005), pp. 197–222.
[21] Note that in the literature, the exact equivalence between these two methods was only established rigorously for the case of a planar surface, but not for a structure of arbitrary geometry, although this is expected from conservation of energy. See Ref. 1 and references therein.
[22] R. Fuchs and F. Claro, Phys. Rev. B **35**, 3722 (1987).
[23] U. Kreibig and M. Vollmer, *Optical Properties of Metal Clusters* (Springer-Verlag, Berlin, 1995).
[24] L. B. Scaffardi, N. Pellegri, O. de Sanctis, and J. O. Tocho, Nanotechnology **16**, 158 (2005).
[25] R. Ruppin, Phys. Rev. B **11**, 2871 (1975).
[26] T. L. Jennings, M. P. Singh, and G. F. Strouse, J. Am. Chem. Soc. **128**, 5463 (2006).
[27] The comparison between the hydrodynamic (H) and the Lindhard-Mermin (LM) models as applied to *total* decay-rate calculations has been studied previously for planar metallic surfaces [see S. Corni and J. Tomasi, J. Chem. Phys. **118**, 6481 (2003)], and for core-shell particles [see R. Chang and P. T. Leung, Phys. Rev. B **73**, 125438 (2006); **75**, 079901(E) (2007)]. While a significant difference between the two models has been observed in the former case, very close results between the two models were obtained in the latter case for a molecule at 1 nm from a metallic nanoshell. The LM model is in principle more accurate than the H model since the latter is simply the lowest order (in wave vector) approximation of the former, and it excludes electron-hole pair excitations in the metal. A detailed comparison between the two models as applied to calculations of each of the fluorescence, radiative, and nonradiative rates will be of interest and will be left for a future endeavor.
[28] A. T. George, Opt. Commun. **188**, 321 (2001).
[29] T. Marniv and H. Metiu, Phys. Rev. B **22**, 4731 (1980); G. E. Korzeniewski, T. Marniv, and H. Metiu, J. Chem. Phys. **76**, 1564 (1982); **76**, 2697 (1982).